

# Unsupervised Capsule Networks of High-Dimension Point Clouds classification

Quanfeng Xu<sup>1</sup>, Zuo Jiang<sup>1</sup>, Yan Yang<sup>2</sup>, Yi Tang<sup>1\*</sup> and Yumei She<sup>1</sup>

<sup>1\*</sup>School of Mathematics and Computer Science, Yunnan Minzu University, 2929 Yuehua Street, Kunming, 650500, China.

<sup>2</sup>School of Mathematics and Statistics, Hubei University of Arts and Science, 296 Longzhong Road, Xiangyang, 441053, China.

\*Corresponding author(s). E-mail(s): [yitang.math@gmail.com](mailto:yitang.math@gmail.com);  
Contributing authors: [xqf3520@163.com](mailto:xqf3520@163.com); [150428967@qq.com](mailto:150428967@qq.com);  
[unicornyy@163.com](mailto:unicornyy@163.com); [sheym1965@126.com](mailto:sheym1965@126.com);

## Abstract

**Background:** Three-dimensional point clouds learning is widely applied, but the point clouds are still unable to deal with classification and recognition tasks satisfactorily in the cases of irregular geometric structures and high-dimensional space. In 3D space, point clouds tend to have regular Euclidean structure because of their density. On the contrary, due to the high dimensionality, the spatial structure of high-dimensional space is more complex, and point clouds are mostly presented in non-Euclidean structure. Furthermore, among current 3D point clouds classification algorithms, Canonical Capsules algorithm based on Euclidean distance is difficult to decompose and identify non-Euclidean structures effectively.

**Methods:** Thus, aiming at the point clouds classification task of non-Euclidean structure in 3D and high-dimensional space, this paper refers to the LLE algorithm based on geodesic distance for optimizing and proposes the unsupervised capsule algorithm of high-dimensional point clouds. In this paper, the geometric features of point clouds are considered in the extraction process, so as to transform the high-dimensional non-Euclidean structure into a lower-dimensional Euclidean structure with retaining spatial geometric features.

**Results:** To verify the feasibility of the unsupervised capsule algorithm of high-dimensional point clouds, experiments are conducted in Swiss Roll dataset, point clouds MNIST dataset and point

clouds LFW dataset. The results show that (1) non-Euclidean structures can be effectively identified by this model in Swiss Roll dataset; (2) a significant unsupervised learning effect is realized in point clouds MNIST dataset; (3) a classification accuracy of 80.77% is obtained in the point clouds LFW dataset.

**Comclusions:** In conclusion, the high-dimensional point clouds capsule unsupervised algorithm proposed in this paper is conducive to expand the application scenarios of current point clouds classification and recognition tasks.

**Keywords:** Capsule Networks, High-dimensional Point Clouds, Geometric Structures, Dimensionality Reduction, Unsupervised Learning, Manifold Learning

## 1 Introduction

Point cloud deep learning techniques have a wide range of applications in computer vision, robot control, autonomous driving etc. Moreover, three-dimensional point clouds retain the spatial geometric information of objects and the spatial structure that RGB pictures do not possess. With the continuous development of deep learning, many 2D computer vision problems have been solved, but the research on deep learning for 3D point clouds and 3D computer vision is far from enough. That research on 3D or high-dimensional point clouds still faces challenges. Thus, studying and solving those challenges is significant for the development of point cloud deep learning.

The existing mainstream deep learning methods for 3D point clouds can be divided into three categories [1]: multi-view-based methods, volumetric-based methods, and point-based methods. Selecting point-based method, Canonical Capsules algorithm [2] implements an unsupervised algorithm for 3D point clouds through reconstructing ShapeNet decomposition of large-scale datasets. Canonical Capsules algorithm effectively learns the regular shape features of point clouds during the classification and reconstruction process, due to the K-Means clustering algorithm based on the Euclidean distance between two points. However, the K-Means clustering merely based on the Euclidean distance not only cannot correctly classify the special two points with small Euclidean distance and large geodesic distance in the point clouds, but also fails to effectively decompose and reconstruct the special non-Euclidean structure of the Swiss Roll dataset.

The recognition and classification algorithm of 3D point clouds has a broad application prospect in computer vision. Further, given the condition that irregularly shaped 3D point cloud objects are inevitable in application, it is significant to classify them accurately for the sake of the future of 3D point clouds in computer vision. What's more, 3D point cloud data can only express or interpret the world in 3D or below, rather than higher dimensional space. In reality, point clouds in higher dimensional space are different from those in

3D space because of their high dimensionality as well as their complexity of geometric and spatial structures, which make it difficult for high-dimensional point clouds to have regular spatial shapes and Euclidean structures. Thus, in this paper, we first utilize the locally linear embedding (LLE) algorithm [3] to optimize the extraction process of model features [4], then transform the irregular non-Euclidean high-dimensional point clouds into Euclidean structure in the lower-dimensional point cloud space, and last deploy the high-dimensional point cloud capsule algorithm to achieve unsupervised learning of Euclidean structure data.

In response to the situation that existing methods cannot effectively verify the geometric spatial structure of 3D point clouds, this paper adds the LLE algorithm when extracting features by the Canonical Capsules algorithm for optimizing, so that the 3D non-Euclidean structure is decomposed correctly and then the significant unsupervised results of high-dimensional point clouds are obtained. 3D point clouds capsule model in Canonical Capsules algorithm is replaced with high-dimensional point cloud capsule model by conducting the input dimension of the model and the random rigid rotation of point clouds as innovation.

Based on the above issues, the main contributions of this paper are:

- (1) The Canonical Capsules algorithm is optimized by adding the LLE algorithm to extract the geometric features of the original data, so that the high-dimensional non-Euclidean structure is transformed into the low-dimensional Euclidean structure.
- (2) The input dimension of the 3D point cloud model and the random rigid rotation matrix of the point cloud are improved to high-dimension, and further the Canonical Capsules algorithm is improved from the 3D point cloud capsule algorithm to the high-dimensional point cloud capsule algorithm.
- (3) The high-dimensional point cloud capsule algorithm is improved to free unsupervised learning of point clouds from 3D point clouds. Based on MNIST dataset in form of point clouds, this paper explores how the model can classify samples with different attributes between category under unsupervised conditions by analyzing the invariance and covariance of features in MNIST dataset. Furthermore, this paper investigates how to utilize point clouds LWF dataset to perform unsupervised classification of face images among different categories.

## 2 Related works

Since Hinton et al. [5] have proposed the concept of auto-encoder capsule networks, this concept has gained popularity since some its advantages over CNNs [6, 7]. Capsule networks are utilized to extract invariant and equivariant features and provide new ideas for pose computation of images and 3D point clouds. In this section, the related stream shape learning, capsule network, and 3D point cloud capsule algorithms utilized in the high-dimensional point cloud capsule algorithm are introduced subsequently.

## 2.1 LLE as Manifold Learning

Locally Linear Embedding [3, 8] is a kind of Manifold Learning. The manifold in LLE can be considered as a non-closed surface, which has a relatively uniform data distribution and dense features. The dimensionality reduction algorithm based on manifold is to reduce the dimensionality of the manifold from high to low dimension. Meanwhile, some features of the manifold in high dimension are preserved.

The manifold learning retains some features of the local structure. There are various methods to retain the features, and different methods correspond to different manifold algorithms. For example, the isometric mapping algorithm maintains the geodesic distance between samples after dimensionality reduction instead of the Euclidean distance, which better reflects the true distance between samples in the manifold. However, the disadvantage of the isometric mapping algorithm is that it searches for the global optimal solution for all samples. That time would be quite long in the case of large data volume and high dimensions. To deal with this problem, LLE reduces the computational effort of dimensionality reduction by guaranteeing merely the local optima and assuming that the sample set is locally in linear relation. The core idea of LLE is that each point can be approximated by a linear combination of multiple points close to it, and this linear reconstruction relationship and reconstruction coefficients should be maintained after being projected to the low-dimensional space.

The LLE for optimizing the n-dimensional point cloud dataset to extract geometric features is operated in the following steps:

The first step of the LLE algorithm is to obtain the k-neighbor points of each data by applying the k-nearest neighbor algorithm. Each sample point  $x_i$  in the point cloud can be represented by a linear combination of the k-nearest neighbor points, where  $Q(i)$  represents the set of k-nearest neighbor samples of point  $x_i$ .

$$x_i = \sum_{j \in Q(i)} \omega_{ij} x_j \quad (1)$$

The second step calculates the reconstruction coefficients. Each sample point  $x_i$  in the point cloud can be linearly represented by its neighbors to obtain the minimum loss sum of n points, which is summarized as follows:

$$\arg \max_W \sum_{i=1}^N (\|x_i - \sum_{j \in Q(i)} \omega_{ij} x_j\|_2^2) \quad (2)$$

The third step is to project geometrical structure in a high-dimensional space into a low-dimensional space. After the original data is reduced from n-dimensional to m-dimensional, it can still be expressed as a linear combination of its k-nearest neighbors, and the combination coefficient remains. The linear combination coefficient between each sample point and its neighbor nodes will be obtained and considered as a known quantity, to solve the following

optimization problem and complete the vector projection as follows (3):

$$\arg \min_Y \sum_{i=1}^N (\|y_i - \sum_{j \in Q(i)} \omega_{ij} y_j\|_2^2) \quad (3)$$

The obtained  $y_i = (y_{i1}, \dots, y_{im})$  can represent the m-dimensional point cloud with geometric features in the whole n-dimensional point clouds of the original point  $x_i = (x_{i1}, \dots, x_{in})$  as well as the remaining geometric and Euclidean structures in the m-dimensional low-dimensional point cloud.

## 2.2 The development of Capsule Networks

After Hinton first proposed auto-encoders capsule networks [5], many scholars have never ceased to investigate capsule networks because of their great potential. Capsule networks regard a set of neurons in a neural network as a capsule, and multiple capsules are combined into a capsule network hidden layer. Further, Sabour et al. [9] proposed a dynamically routed capsule networks, which merged two layers of capsules for the first time, called CapsNet. It achieves better classification effect than CNN on MNIST. In other words, dynamic routing protocol equips the capsule networks with functions that CNN do not have to achieve effective classification on MultiMNIST. Moreover, the EM routing [10] proposed by Hinton in 2018 adds the maximum likelihood estimation algorithm to routing by representing a capsule with pose matrix and activation probability and activating the next higher-level capsule with dynamic routing. Later, Ribeiro et al. [11] introduced the Bayesian estimation algorithm to routing to optimize the parameters transfer rule between capsules by variational Bayes. The feature maps in Capsule networks differ from that in CNN in that dynamic weight transfer is composed of primary and higher-level capsules. It has been verified by Venkatraman et al. [12] that protocol routing mechanism is the key to the composition of capsule networks.

The research on capsule networks has developed rapidly in recent years, and capsule networks have gradually emerged in a variety of deep learning tasks [13–20]. Because of their great potential, they have been widely used in natural language processing [21, 22], computer vision, medicine and other fields. More importantly, capsule networks could and have been combined with 3D point cloud machine learning. The dynamic routing structure of capsule networks can divide the pose and other attributes of 3D point clouds into invariant and equivariant features for subsequent learning, which takes better use of that information of point clouds compared with CNN. The method adopted in this paper upgrades it from a 3D point cloud algorithm to a high-dimensional point cloud algorithm. In this paper, the three-dimensional point clouds algorithm is extended to the high-dimensional space, thus breaking through the three-dimensional limitation. In addition, LLE algorithm is added to preserve the spatial structure of the high-dimensional point clouds, so that the low-dimensional point cloud still retains its spatial geometric structure and realizes the classification of the high-dimensional point clouds.

## 2.3 Capsules networks for 3D Point Clouds

The 3D point clouds with geometric capsule auto-encoders [23] proposed by Nitish Srivastava in 2019 is based on a multi-view approach. This model indicates that learning interpretable geometric representations is feasible for machines and multi-view protocols contribute a lot to this feasibility. The multi-view protocol algorithm proposes canonical pose and pose invariance, which effectively solves the task of point clouds alignment and retrieval. This capsule network design addresses how to handle multiple valid interpretations of an object by top-down information. In other words, the object-level capsule activates a lower-level capsule in the decoder to examine these points. The method of voting for object capsules by geometric capsules using pose and feature is derived from EM routing capsules [10]. This method applies the capsule networks to the multi-view pictures to describe the 3D structure of the point cloud, but for the entire 3D structure, the multi-view only expresses very limited pose content and fails to comprehensively reveal the spatial structure and pose of the 3D point clouds.

The Canonical Capsules algorithm [2] proposed by Sun Weiwei in 2020 is a completely unsupervised learning method based on points of 3D-point clouds, which truly achieves completely unsupervised learning on large-scale datasets. This algorithm decomposes the point cloud by k-folds to obtain the primary capsules, and then used those primary capsules to estimate the invariant shape of the point clouds and the covariance of each part of the point clouds center. By associating the capsule pose with the capsule shape (invariance), an object-centered coordinate framework is constructed to support the subsequent auto-encoders network. Its unsupervised learning on the ShapeNet dataset and accuracy outperform both the AtlasNetV2 network [23] and the 3D-PointCapsNet network [24]. This algorithm is based on points to apply the capsule network to 3D point clouds, which can effectually compensate for the defects of geometric capsules. However, the decomposition and reconstruction of point clouds with the irregular spatial structure are not satisfactory.

Deep learning of 3D point clouds contains three main tasks: 3D shape classification [25–29], 3D targets detection and tracking [30–32], and 3D point cloud separation [33, 34]. The Canonical Capsules algorithm proposed by Sun Weiwei uses the features of each part from decomposing and reconstructing 3D point clouds for classification.

In the Canonical Capsules algorithm for decomposing and reconstructing 3D point clouds, the eleven categories of 3D models, such as the models of airplanes, benches and tables with smooth surfaces and regular spatial structures, are well decomposed into individual parts as shown in Figure 1. The unsupervised clustering of features of individual parts subsequently assists in judging the feature point, which is used to determine which feature part of the point clouds a point is located in and further to decide the category of the whole point cloud based on the presence of those parts.

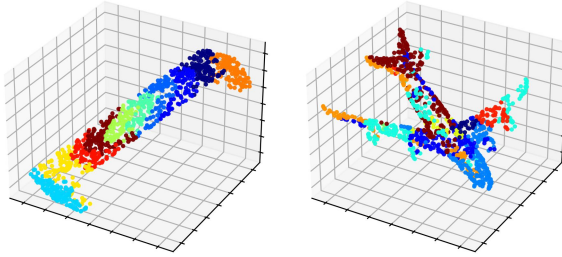


**Fig. 1** Examples of decomposing point clouds (a bench on the left, and a plane on the right)

### 3 High-Dimensional Point Clouds Capsule Model

Compared with CNN networks which can only determine the presence or absence of features, capsule networks are able to use their features' invariance and equivariance. Thus, an improved capsule network-based algorithm for high-dimensional point clouds should include this ability to distinguish between invariance and equivariance of point cloud data features. In this section, the network structure of the Canonical Capsules algorithm is ameliorated to that of high-dimensional point clouds, and the original network that can only operate in two and three dimensions is transformed into a network that can operate on high-dimensional point clouds. The improvement aspects of model network structure include dimension of point cloud input and high-dimensional point cloud loss function in Section 3.1, as well as rigid rotation change of point cloud in Section 3.2.

#### 3.1 Input and Loss of High-Dimensional Point Clouds

As for the 3D point clouds input in the original model, the input is processed in high dimensions. Specially, a given point cloud  $P \in R^{(X \times D)}$  denoting  $x$  points in the  $D$  dimension make up these point clouds  $P$ , is transformed into  $k$  capsules  $A \in R^{(X \times K)}$  and  $c$  channels for each point  $F \in R^{(X \times C)}$  by autoencoders, which could be placed in the following equation (4).

$$\theta_k = \frac{\sum_p A_{p,k} P_p}{\sum_p A_{p,k}}, \beta_k = \frac{\sum_p A_{p,k} F_p}{\sum_p A_{p,k}} \quad (4)$$

In this equation,  $\theta_k \in R^D$  denotes the pose of the  $k^{th}$  capsule and its position parameter in  $D$ -dimensional space, and the corresponding capsule shape information  $\beta_k \in R^C$ . The position parameter  $\theta_k$  has spatial equivariance and can be realized after rotation and translation. The  $\beta_k$  denotes the shape information of the point clouds which is invariant. Then,  $\theta_k$  and  $\beta_k$  are used to calculate the loss of their invariance and equivariance, and the features are divided into invariance and equivariance in the encoder, but the invariance and

covariance of their features are combined again in the subsequent decoding process to generate the decomposed and reconstructed point clouds.

The loss of the 3D point cloud in the Canonical Capsules algorithm is twofold. After two random rigid rotational changes, the point cloud  $P \in R^{(X \times D)}$  becomes two different point clouds  $T^a(P)$  and  $T^b(P)$  via different random rigid rotations  $T^a$  and  $T^b$ . The autoencoder calculates the  $\theta_k$  equivariant and  $\beta_k$  invariant as follows (5).

$$A_a, F_a = \text{Encoder}(T^a(P)) \quad (5)$$

Using the acquired  $A^a, F^a$ , then  $\theta_k^a$  and  $\beta_k^a$  are calculated by the equation (6).

$$\theta_k^a = \frac{\sum_p A_{p,k}^a P_p^a}{\sum_p A_{p,k}^a}, \beta_k^a = \frac{\sum_p A_{p,k}^a F_p^a}{\sum_p A_{p,k}^a} \quad (6)$$

The equivariance loss and invariance loss are calculated after rotating the results of two rigid rotation. The  $\theta_k$  represents equivariance of the capsule indicating its position information. The value of  $\theta_k^b$  after first inverse rotation  $(T^b)^{-1}$  approaches to that of the origin cloud. Moreover, after the second rigid rotation  $T^a$  is completed, its value approaches to that of the original point cloud rotated by  $T^a$ . The invariance of the capsule  $\beta_k$  should remain constant after rotation even including random rigid rotation. The loss of the two rigid rotations is calculated as follows (7) and (8).

$$L_{equ} = \frac{1}{k} \sum_k \|\theta_k^a - (T^a)(T^b)^{-1}\theta_k^b\|_2^2 \quad (7)$$

$$L_{inv} = \frac{1}{k} \sum_k \|\beta_k^a - \beta_k^b\|_2^2 \quad (8)$$

The high-dimensionality of this twofold loss enable the loss function to be high-dimensional, and the subsequent losses are all operated according to the high-dimensionality of point clouds input as well as the above invariance and covariance. The error backpropagation of this loss function performed in the high-dimensional point clouds capsule model realize the effective unsupervised learning of the high-dimensional point cloud capsule algorithm.

### 3.2 Rigid Transformations of High-Dimensional Point Clouds

The linear variation of the 3D point clouds could be geometrically expressed as the rotation and translation of the 3D point clouds. The first step is to multiply the point cloud by the 3D orthogonal matrix. In the second step, the translation and rotation of the 3D point clouds are improved to that of the high-dimensional point clouds by changing the 3D orthogonal matrix to a high-dimensional orthogonal matrix.

In the Canonical Capsules algorithm, two random rigid rotational changes to the point cloud are performed, noted as  $T^a$  and  $T^b$ . In the Canonical



Capsules algorithm, this random rotation matrix is rotated to three angles according to the three  $XYZ$  axes respectively  $\alpha$ ,  $\beta$  and  $\gamma$  as shown in Figure 2 below and then  $xyz$  axes are obtained.

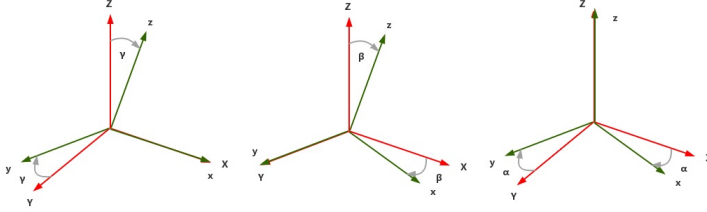


**Fig. 2** Coordinate axis rotation (rotating  $\gamma$  degrees around X-axis on the left,  $\beta$  degrees around Y-axis in the middle,  $\alpha$  degrees around Z-axis on the right)

Three three-dimensional rotation matrices are calculated based on three rotation angles as follows (9):

$$\begin{aligned} R_z(\alpha) &= \begin{pmatrix} \cos \alpha & -\sin \alpha & 0 \\ \sin \alpha & \cos \alpha & 0 \\ 0 & 0 & 1 \end{pmatrix}, \\ R_y(\beta) &= \begin{pmatrix} \cos \beta & 0 & \sin \beta \\ 0 & 1 & 0 \\ -\sin \beta & 0 & \cos \beta \end{pmatrix}, \\ R_x(\gamma) &= \begin{pmatrix} 1 & 0 & 0 \\ 0 & \cos \gamma & -\sin \gamma \\ 0 & \sin \gamma & \cos \gamma \end{pmatrix}. \end{aligned} \quad (9)$$

Based on three above matrices, matrix multiplication is performed to obtain the rotation matrix of the 3D point clouds rigid rotation as described in the following equations (10).

$$R(\alpha, \beta, \gamma) = R_z(\alpha)R_y(\beta)R_x(\gamma) \quad (10)$$

The random rigid transformation matrix of the three-dimensional point clouds is as above. However, the rotation of the high-dimensional space beyond three dimensions, is hard to be expressed by trigonometric functions, and the rotation in high-dimensional form is more difficult to be reflected by rotation relationships between each axis. The random rigid rotation in this paper selects two linearly independent high-dimensional unit vectors  $\vec{a}$  and  $\vec{c}$  in the  $n$ -dimensional space to construct the rotation matrix [35] in the high-dimensional space. In that matrix,  $A = [\vec{a}, \vec{c}]$  is the matrix of size  $n \times 2$  and any given  $\vec{x}$

vector will be decomposed into two parts as shown in (11).

$$\vec{x} = x_{\perp} + x_{\parallel} \quad (11)$$

$$x_{\perp} = A(A^T A)^{-1} A^T \vec{x} \quad (12)$$

$$x_{\parallel} = (I - A(A^T A)^{-1} A^T) \vec{x} \quad (13)$$

Some  $x_{\perp}$  is perpendicular to the plane formed by the two-unit vectors  $\vec{a}$  and  $\vec{c}$ , and  $x_{\parallel}$  is parallel to the plane formed by the two-unit vectors  $\vec{a}$  and  $\vec{c}$ . It can be derived that (12) and (14). After rotating the  $\vec{x}$  from  $\vec{a}$  and  $\vec{c}$ , the change can be obtained as below in (14),

$$\vec{x}' = x_{\perp} + x'_{\parallel} \quad (14)$$

where the rotation from  $\vec{a}$  to  $\vec{c}$  does not change the  $x_{\perp}$  vector, but only affects the  $x_{\parallel}$  vector. This rotation from  $\vec{a}$  to  $\vec{c}$  can be described as the matrix as (15).

$$\begin{bmatrix} 0 & -1 \\ 1 & 2(\vec{a} \cdot \vec{c}) \end{bmatrix} \quad (15)$$

Further, (14) could be derived from (13).

$$x'_{\parallel} = A \begin{bmatrix} 0 & -1 \\ 1 & 2(\vec{a} \cdot \vec{c}) \end{bmatrix} (A^T A)^{-1} A^T \vec{x} \quad (16)$$

To obtain the rotation matrix, (13) and (16) are substituted into (14) to get (17).

$$\begin{aligned} \vec{x}' &= A \begin{bmatrix} 0 & -1 \\ 1 & 2(\vec{a} \cdot \vec{c}) \end{bmatrix} (A^T A)^{-1} A^T \vec{x} \\ &\quad + (I - A(A^T A)^{-1} A^T) \vec{x} \end{aligned} \quad (17)$$

In short, the matrix representation of its rotation process from  $\vec{a}$  to  $\vec{c}$  in the high-dimensional space is concluded in (18):

$$I + A \left( \begin{bmatrix} 0 & -1 \\ 1 & 2(\vec{a} \cdot \vec{c}) \end{bmatrix} - I_{2 \times 2} \right) (A^T A)^{-1} A^T \vec{x} \quad (18)$$

The rotation matrix of rigid transformation in high-dimensional point cloud space is obtained, and the random rigid translational rotation of high-dimensional space is performed. Thus, the limitation that trigonometric functions cannot effectively reflect random rotation in high-dimensional space is solved, and the random rigid rotation matrix of the point clouds in high-dimensional space can be rapidly calculated.

## 4 Results

To verify the classification efficiency of the high-dimensional point clouds capsule model on the point clouds data with high-dimensional non-Euclidian structure, experiments in the Swiss Roll dataset, point clouds MNIST dataset and LFW dataset are conducted. First, since the unsupervised classification effect of Canonical Capsules algorithm on 3D non-Euclidian structures is not significant, this paper selects the high-dimensional point clouds capsule model optimized by LLE algorithm in Section 4.1. Second, the high-dimensional non-Euclidian structure point clouds model optimized by LLE is used to identify and classify handwritten numeral images in point clouds MNIST datasets in Section 4.2. Finally, this paper compares the classification accuracy of this model on natural face images with high-dimensional non-European structure after different dimensionality reduction methods and quantity in Section 4.3.

### 4.1 The model in clustering Swiss Roll Dataset

Since the Canonical Capsules algorithm could not achieve effective clustering on the Swiss Roll dataset, the LLE algorithm is added to extract features. On the basis of Canonical Capsules algorithm, LLE algorithm is used to extract geometric features of 3D non-Euclidean structures in 2D space, and 3D point clouds are extended to higher-dimensional space. In that high-dimensional space, this paper further tests the effect of the high-dimensional point clouds capsule model optimized by LLE in unsupervised decomposition and reconstruction tasks.

#### 4.1.1 Canonical Capsules Algorithm for clustering

The point cloud structure in three-dimensional space does not necessarily possess a regular spatial structure and smooth surface. Its original structure is shown in the left of Figure 3, and the Canonical Capsules algorithm operation results in the right. which can be found that the original algorithm based on K-means clustering cannot effectively decompose its structure in unsupervised situations. The LLE algorithm is introduced to improve the original algorithm

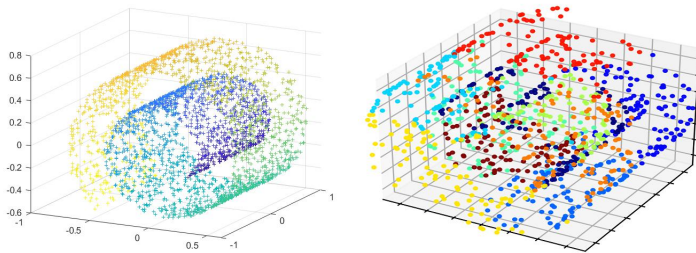


**Fig. 3** Decomposing the point clouds of Swiss Roll dataset (Original image on the left, calculation result on the right)

which cannot effectively cluster the 3D geometric structure with K-Means. In LLE, the geometric features from the Swiss Roll dataset are extracted and passed into the model together with the original point clouds data so that this model takes into account the geometric structure of the point cloud in the meantime. Moreover, LLE includes not only Euclidean distance considered by K-means clustering, but also geodesic distance. By improving non-Euclidean structures in 3D space, better unsupervised learning results can be achieved.

#### 4.1.2 The model for clustering

By LLE algorithm, the original three-dimensional point  $x_i = (x_{i1}, x_{i2}, x_{i3})$  is transformed into a two-dimensional point  $y_i = (y_{i1}, y_{i2})$  containing the original geometric structure, and then that two-dimensional point is combined with the original three-dimensional point cloud data. Thus, the high-dimensional point cloud  $(x_{i1}, x_{i2}, x_{i3}, y_{i1}, y_{i2})$  is formed. The process of putting Swiss Roll dataset into the model is shown in the flow chart Figure 4.

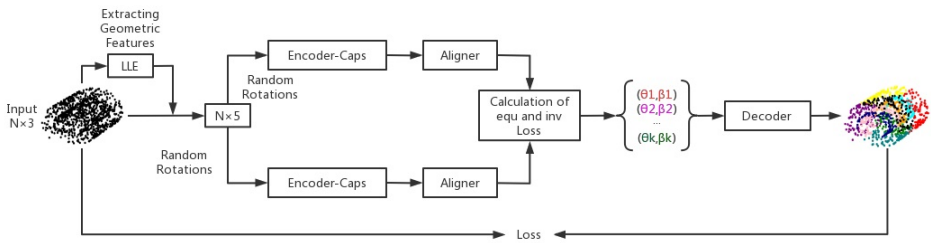


**Fig. 4** Swiss Roll dataset in high-dimensional point cloud capsule model

After the geometric features of the Swiss Roll dataset plus the original 3D point cloud data are synthesized into high-dimensional coordinates and then calculated by the high-dimensional point clouds capsule model, the visualization results are obtained in Figure 5. In the figure, unclassified Swiss Roll point clouds are in the first row, classified Swiss Roll point clouds are in the second row, and classified Swiss Roll point clouds on the 3D axis are in the third row.

As demonstrated in Figure 5, this model with LLE algorithm is able to identify the relationship between different parts of Swiss Roll dataset effectively. In other words, the LLE-optimized model has the feasibility of correctly decomposing and classifying high-dimensional non-Euclidean point clouds. The LLE combines with the Canonical Capsules algorithm to convert the non-Euclidean structure in high-dimensional space into low-dimensional Euclidean structure, retaining the geometric features of high-dimensional point clouds for unsupervised learning. On the contrary, the Canonical Capsules algorithm cannot effectively classify the 3D non-Euclidean structure and is not suitable

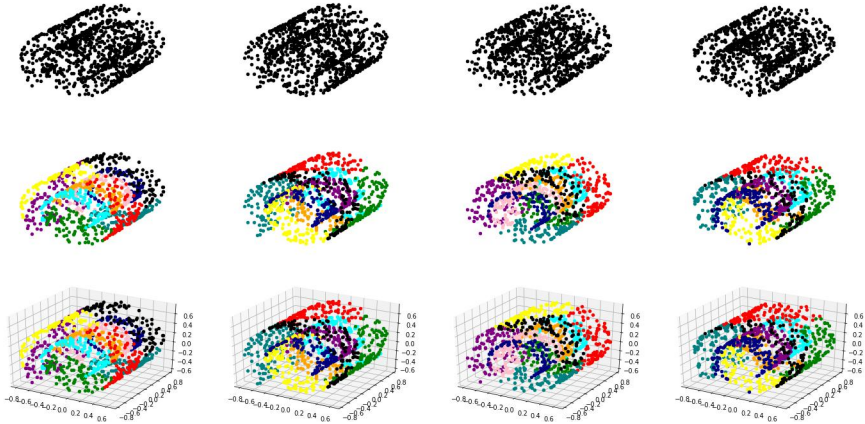


**Fig. 5** Visualized training results of the Swiss Roll in LLE optimized high-dimensional point clouds model

for more complex higher-dimensional spaces as well as non-Euclidean structures. Thus, the introduction of the LLE algorithm could retain the geometric structure of non-Euclidean structures in high-dimensional space to the low-dimensional space of Euclidean structures, which is of great significance for effective unsupervised classification of point clouds in high-dimensional space.

## 4.2 Classification of model in Point Cloud MNIST dataset

To test whether the high-dimensional point clouds capsule model can effectively extract spatial features and unsupervised learning from the authentic high-dimensional non-Euclidean structure data, the MNIST dataset is transformed into the point clouds MNIST dataset for the experiment.

### 4.2.1 Preparing Point Clouds MNIST Dataset

MNIST is a classical computer vision dataset in which images are composed of  $28 \times 28$  pixels. A single MNIST image can be viewed as a  $28 \times 28$  matrix, and the value at the corresponding position is the degree of lightness or darkness of that pixel point as shown in Figure 6. Since each of these values describing the degree of lightness and darkness could be considered as a vector of dimensions, a single MNIST image can be equivalently transformed into a point in a  $784(28 \times 28)$ -dimensional space.

MNIST is necessarily contained in this high 784-dimensional space, and further this space can contain any  $28 \times 28$ -pixel pictures, such as in Figure 7 an image generated after randomizing the value of each pixel in  $28 \times 28$ . After inference and analysis, it is not difficult to find that the features and information that can be expressed in the 784-dimensional space are much larger compared to that of MNISTs.

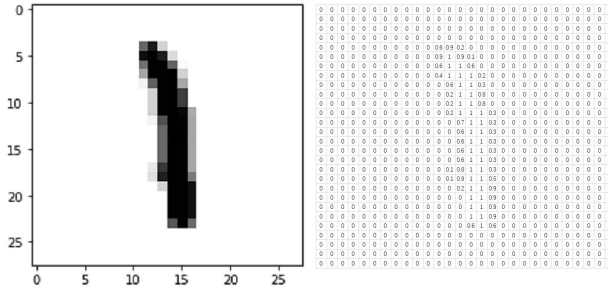


**Fig. 6** MNIST image (original on the left, numerical on the right)

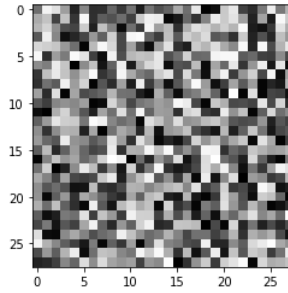


**Fig. 7** A 28×28 pixel randomly generated image

Although MNIST is embedded in the 784-dimensional space, it only occupies a very small part of the subspace. If it performs gradient descent directly in the 784-dimensional point cloud, the initial value point is likely to be selected to the 784-dimensional space beyond MNIST, and then it is difficult to find a reasonable initial value point to complete gradient descent. Therefore, the LLE algorithm needs to be introduced first for dimensionality reduction. The MNIST dataset of point clouds after dimensionality reduction is used to randomly select points to form multiple point sets.

#### 4.2.2 Classifying Point Clouds MNIST Dataset

The 784-dimensional point cloud is downsampled by LLE to retain its high-dimensional spatial geometric features while achieving Euclidean spatial structure. Since the essential dimension of the point cloud MNIST data set cannot be accurately and conveniently derived, another more appropriate way is to find its effective dimension by adopting the exhaustive example method. The 784-dimensional point cloud transformed from the MNIST dataset cannot descend in a gradient after being put into the high-dimensional point cloud capsule model, because MNIST only occupies a small low-dimensional subspace in the 784-dimensional space. Thus, 784-dimensions cannot be effectively gradient-descended without dimensionality reduction. Even when the dimensionality is reduced to 36 dimensions, 784-dimensions still cannot be

effectively gradient-descended. The gradient-descending is carried out until the exhaustive enumeration down to 14-dimensions, and the loss value of gradient-descending is calculated. The above procure is presented in Figure 8.

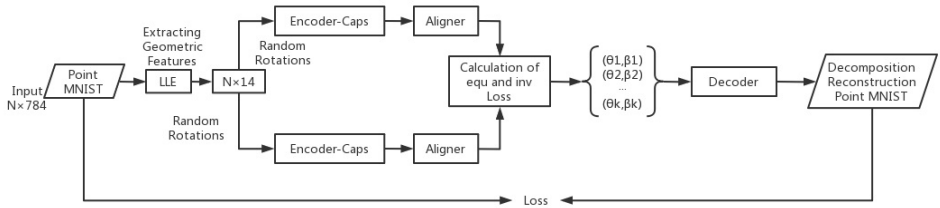


**Fig. 8** Point cloud MNIST

Further, the 784-dimensional point clouds of the same category are down-scaled into 14-dimensional point clouds by the LLE algorithm and then imported into the high-dimensional point cloud capsule model for decomposition and reconstruction. The features of the same category of MNIST are unsupervised learned through the model with  $\theta_k \in R^{14}$  indicating the position parameters of the  $K^{th}$  capsule in the 14-dimensional space and  $\beta_k \in R^C$  indicating its corresponding capsule shape information. The features of each similar part of the same category are effectively clustered without supervision by the K-Means clustering based on Euclidean distance between points and the LLE algorithm based on geodesic distance.

After images in MNIST with label "1" are selected, the visualization of MNIST dataset decomposition results and PCA dimensionality reduction of point cloud are shown in Figure 9 below. In the figure, different categories have clear dividing lines which can be used for follow-up studies to explore the relationship of subspaces.

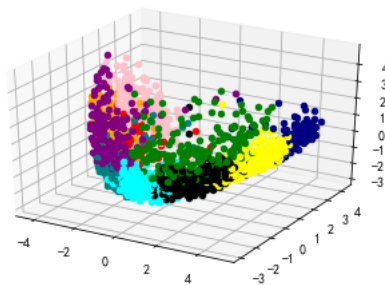


**Fig. 9** Dimensionality reduction of MNIST point clouds

From Figure 9, it is easy to see that the "1" category of the MNIST dataset with obvious high-dimensional geometric boundaries, still has a clear

performance after its dimensionality reduction. The subspaces occupied by various features have their own roles in controlling the morphology of the "1". The results of tracing the points in each category back to the 28×28 MNIST handwritten picture are visualized in Figure 10.

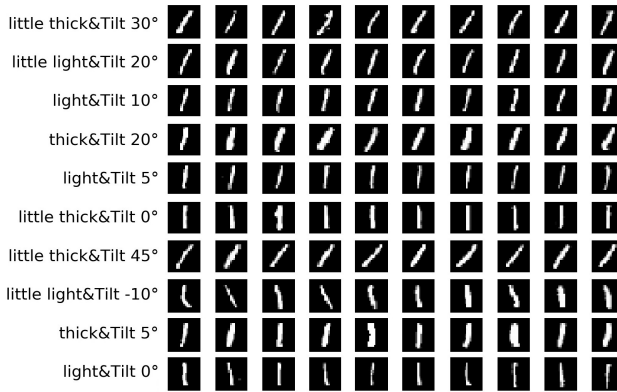


**Fig. 10** Visualization results of MNIST point clouds

Figure 10 shows the 100 MNIST images of "1". The same category is put in the same row. And within each row the unsupervised learning results of the point cloud are presented. The top three rows are tilted clockwise, and their thickness varies: The first row is thicker and tilted 30°, the third row is thin and tilted 10°, and the second row is in between. The thickness of the handwritten numeral in the fourth line is more obvious and inclined at 0°. The figures in the fifth, sixth, ninth, and tenth rows are closer to the vertical state, but with different thickness and tilt characteristics. The seventh line is tilted at a pronounced clockwise angle. The eighth row is tilted to the counterclockwise angle. Based on what was discussed above, the high-dimensional point clouds capsule model classifies such handwritten numbers "1" into 10 categories according to their characteristics in an unsupervised way.

The capsule network realizes label-free clustering of MNIST images of the same category according to their morphology, thickness and other characteristics through comprehensive consideration of invariance and covariance of data set. It performs better than CNN network which can only distinguish the presence or absence of certain categories, and provides strong support for further studies on invariance and equivariance characteristics of, morphology, thickness and tilt degree.



### 4.3 Accuracy of the model in point clouds LFW dataset

To explore the effect of dimension reduction method and degree on the high-dimensional point clouds capsule model and to test whether the high-dimensional point clouds capsule model can perform effective unsupervised learning on the high-dimensional non-Euclidean point clouds data transformed from natural pictures, the following experiments are conducted. This paper first takes out the top 10 images in LFW data set. If the frequency of the image is too low, data enhancement is performed. Then, the images are transformed into point clouds LFW data set to carry out unsupervised classification experiments.

#### 4.3.1 Classifying point clouds LFW dataset

The LFW dataset is closer to the real natural pictures than the monochrome MNIST dataset, where the unconstrained facial image in a natural setting is composed of  $62 \times 47$  pixels. A single picture of the LFW dataset can be viewed as a point in 2914-dimensional space. As mentioned in Section 4.2.1, it is difficult to perform effective gradient descent in the high-dimensional space, so the 2914-dimensional points are subjected to LLE for dimensionality reduction. The 2914-dimensional point cloud is downscaled by LLE, and the degree of dimensionality reduction is referred to Section 4.2.2. After dimensionality reduction to 14 dimensions, effective gradient descent is conducted. The whole procedure is summarized in Figure 11.

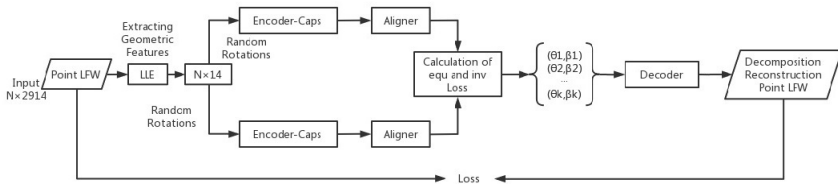


**Fig. 11** high-dimensional point clouds of LFW in capsule model

The point cloud for extracting geometric features is decomposed into individual parts. Further, the unsupervised learning results of the loss in each part are compared with the real labels to evaluate point clouds in extracting features and learning.

The face clustering results of two people in the excerpted dataset are reported in Figures 12 and 13.

The unsupervised learning is performed with the high-dimensional capsule network. Moreover, the learning outcome is compared with the true labels and then the confusion matrix is obtained in Figure 14.

From the confusion matrix in Figure 14, it can be seen that the classification accuracy reaches 80.77%. This high accuracy indicates that the



**Fig. 12** Clustering effect of Ariel Sharon's face images in LFW dataset



**Fig. 13** Clustering effect of Colin Powell's face images in LFW dataset

high-dimensional point cloud capsule model has the excellent ability to extract and discriminate the features contained in the high-dimensional points, as well as to classify natural images. The point clouds LFW dataset utilizes the capsule network and combines invariance and equivariance to classify each feature within category first and then to complete classification between categories.

#### 4.3.2 Comparing accuracy by two deduction methods: PCA and LLE

To verify the performance of LLE optimization, the high dimensions are reduced to 14 and 3 in the way of LLE and PCA respectively. The comparison of this model's unsupervised classification performance for high-dimensional point clouds in different contexts are shown in Table 1 below.

From the above four experiments, it can be seen that the accuracy of PCA dimension reduction is much lower than that of LLE dimension reduction while the loss of PCA dimension reduction is much higher. It indicates that LLE can effectively downscale the high-dimensional point clouds with non-Euclidean structures containing spatial geometric information to low-dimensional point clouds with Euclidean structures. Moreover, LLE optimization is able to make the clutter high-dimensional spatial information effectively identified in the low-dimensional space by the unsupervised point cloud that can only identify

|        |                   |           |     |     |     |     |     |     |     |     |     |
|--------|-------------------|-----------|-----|-----|-----|-----|-----|-----|-----|-----|-----|
| Actual | John Ashcroft     | 79%       | 2%  | 2%  |     | 6%  |     |     |     | 11% |     |
|        | Jean Chretien     | 5%        | 73% | 4%  |     |     | 5%  |     | 2%  | 11% |     |
|        | Junichiro Koizumi |           | 3%  | 85% |     |     | 3%  | 3%  |     | 3%  | 2%  |
|        | Hugo Chavez       | 4%        | 1%  |     | 80% |     | 1%  | 6%  | 1%  | 3%  | 3%  |
|        | Ariel Sharon      | 5%        | 3%  | 1%  | 4%  | 73% | 1%  | 1%  | 3%  | 8%  | 1%  |
|        | Gerhard Schroeder | 6%        | 5%  | 4%  | 2%  |     | 74% | 1%  |     | 6%  | 3%  |
|        | Donald Rumsfeld   | 3%        | 2%  | 2%  | 2%  | 1%  | 2%  | 79% | 1%  | 7%  |     |
|        | Tony Blair        | 3%        | 3%  | 4%  |     |     | 2%  | 1%  | 83% | 2%  | 1%  |
|        | Colin Powell      | 5%        | 2%  | 1%  | 3%  | 1%  | 1%  |     | 1%  | 85% | 1%  |
|        | George W Bush     | 5%        | 1%  | 1%  | 2%  | 1%  | 1%  | 2%  | 3%  | 4%  | 82% |
|        |                   | Predicted |     |     |     |     |     |     |     |     |     |

**Fig. 14** Confusion matrix of LWF dataset in capsule model

the Euclidean structure algorithm. It is also observed that the loss in three dimensions is less than that in high dimensions, because the high dimensionality leads to its spatial structure is complex and difficult to differentiate. In addition, the accuracy and loss of dimensionality reduction to 3 dimensions is not as great as that of dimensionality reduction to 14 dimensions. This could be explained by the poor capacity of low-dimensional space carries too much information of high-dimensional space. In the process of dimensionality reduction, the essential dimension of the high-dimensional point cloud dataset cannot be calculated, and can only be estimated by the exhaustive method. In short, the degree of dimensionality reduction should not be too large or too small, and as close to the essential dimension as possible, to achieve better performance. The classification accuracy on natural images of the high-dimensional

**Table 1** Comparison of experimental accuracy among four groups.

| No. | Methods    | Dimensionality | Accuracy | Loss    |
|-----|------------|----------------|----------|---------|
| 1   | <i>PCA</i> | 3              | 28.35%   | 0.15019 |
| 2   | <i>LLE</i> | 3              | 49.10%   | 0.00025 |
| 3   | <i>PCA</i> | 14             | 57.25%   | 0.50538 |
| 4   | <i>LLE</i> | 14             | 80.77%   | 0.00164 |

point cloud capsule model optimized by LLE is not low, indicating that the

high-dimensional point cloud learning task is of practical application for realistic 2D computer vision tasks and video classification tasks. Currently, the research of deep learning on point clouds has continuously developed, and the significance of deep learning on high-dimensional point clouds has far-reaching implications for various categories of machine learning tasks without doubt. The addition of capsule networks makes the classification of neural networks more advantageous compared with CNN networks. In short, the research of high-dimensional point clouds in the deep learning of capsule networks has significant implications for a variety of real-world tasks.

## 5 Conclusions and future work

In this paper, we achieve the correct decomposition of point clouds in 3D non-Euclidean space and extend the unsupervised classification algorithm of 3D point clouds to high-dimensional space. In this paper, high-dimensional non-European structural data are successfully transformed into low-dimensional Euclidean structural data to achieve effective unsupervised learning of high-dimensional point clouds when the LLE algorithm is used and preserving geometric features.

The significant unsupervised classification effect in the point clouds MNIST dataset shows that LLE-optimized high-dimensional point cloud capsule model can effectively recognize and classify high-dimensional non-Euclidean structures. Furthermore, the highly accurate classification of the point clouds LFW dataset transformed by natural pictures demonstrates that the high-dimensional point clouds classification task has broad application prospects in real-life deep learning tasks. Meanwhile, this paper explores the influence of different dimensionality reduction methods and degrees on the classification accuracy, and the results show that the high-dimensional point cloud capsule model optimized by manifold learning has advantages.

Conducting point clouds unsupervised classification of natural images in this paper is an innovation that transforms machine learning tasks of natural image classification into point clouds unsupervised learning tasks. This paper indicates that the learning tasks of point clouds can cover various real-life machine learning tasks and the combination of invariance and equivariance of capsule networks is of great use for unsupervised classification. However, future studies still could be carried out from following aspects:

(1) The essential dimensions of a certain point clouds dataset after being transformed is worthy of further investigation.

(2) In the above experiments, the neural network distinguishes invariance and equivariance of high-dimensional point cloud features in the encoding process and fuses them together in the decoding process to realize the reconstruction goal. Further studies can distinguish their invariance and equivariance, and investigate whether it is effective to transfer their equivariance learning to other types of MNIST.

(3) Researchers can explore the spatial structure of high-dimensional point clouds in high-dimensional space, analyze the relationship of each feature in its subspace, as well as the corresponding linear or non-linear relationships, invariance and equivariance are related in its subspace.

## Declarations

**Funding** This study was funded by National Natural Science Foundation of China (Grant number 61866040).

**Ethical approval** This article does not contain any studies with human participants or animals performed by any of the authors.

**Informed Consent** Informed consent was not required as no humans or animals were involved.

**Conflicts of interest** The authors declare that they have no conflict of interest.

## References

- [1] Guo Y, Wang H, Hu Q, Liu H, Liu L, Bennamoun M. Deep Learning for 3D Point Clouds: A Survey. *IEEE Transactions on Pattern Analysis and Machine Intelligence*, vol. 43, no. 12, pp. 4338-4364, 1 Dec. 2021.
- [2] Sun W, Tagliasacchi A, Deng B, Sabour S, Yi KM. Canonical Capsules: Unsupervised Capsules in Canonical Pose. *Thirty-fifth Conference on Neural Information Processing Systems*. 2020.
- [3] Roweis Sam T, Saul Lawrence K. Nonlinear Dimensionality Reduction by Locally Linear Embedding. *Science*. 2000;290(5500):2323-2326.
- [4] Chen S-B, Tian X-Z, Ding CHQ, Luo B, Liu Y, Huang H, et al. Graph Convolutional Network Based on Manifold Similarity Learning. *Cognitive Computation*. 2020;12(6):1144-1153.
- [5] Hinton GE, Krizhevsky A, Wang SD. Transforming auto-encoders. *International conference on artificial neural networks*: Springer; 2011. p. 44-51.
- [6] Chua LO, Roska T. The CNN paradigm. *IEEE Transactions on Circuits and Systems I: Fundamental Theory and Applications*. 1993;40(3):147-156.

- [7] Roska T, Chua LO. The CNN universal machine: an analogic array computer. *IEEE Transactions on Circuits and Systems II: Analog and Digital Signal Processing*. 1993;40(3):163-173.
- [8] Chang H, Yeung D-Y. Robust locally linear embedding. *Pattern Recognition*. 2006;39(6):1053-1065.
- [9] Sabour S, Frosst N, Hinton GE. Dynamic routing between capsules. *Advances in Neural Information Processing Systems* 30. 2017.
- [10] Hinton GE, Sabour S, Frosst N. Matrix capsules with EM routing. *International conference on learning representations*. 2018.
- [11] Ribeiro FDS, Leontidis G, Kollias S. Capsule Routing via Variational Bayes. *Proceedings of the AAAI Conference on Artificial Intelligence*. 2020. p. 3749-3756.
- [12] Venkatraman SR, Anand A, Balasubramanian S, Sarma RR. Learning Compositional Structures for Deep Learning: Why Routing-by-agreement is Necessary. 2020.
- [13] Jaiswal A, AbdAlmageed W, Wu Y, Natarajan P. CapsuleGAN: Generative Adversarial Capsule Network. 2018.
- [14] Nguyen HH, Yamagishi J, Echizen I. Capsule-forensics: Using Capsule Networks to Detect Forged Images and Videos. *ICASSP 2019 - 2019 IEEE International Conference on Acoustics, Speech and Signal Processing (ICASSP)2019*. p. 2307-2311.
- [15] Rosario VMd, Borin E, Breternitz M. The Multi-Lane Capsule Network. *IEEE Signal Processing Letters*. 2019;26(7):1006-1010.
- [16] Xiong Y, Su G, Ye S, Sun Y, Sun Y. Deeper Capsule Network For Complex Data. *2019 International Joint Conference on Neural Networks (IJCNN)2019*. p. 1-8.
- [17] Yang Z, Zhang J, Meng F, Gu S, Feng Y, Zhou J. Enhancing Context Modeling with a Query-Guided Capsule Network for Document-level Translation. 2019.
- [18] Yang S, Lee F, Miao R, Cai J, Chen L, Yao W, et al. RS-CapsNet: An Advanced Capsule Network. *IEEE Access*. 2020;8:85007-85018.
- [19] Huang W, Zhou F. DA-CapsNet: dual attention mechanism capsule network. *Scientific Reports*. 2020;10(1):11383.
- [20] Edraki M, Rahnavard N, Shah M. SubSpace Capsule Network. *Proceedings of the AAAI Conference on Artificial Intelligence*.

2020;34(07):10745-10753.

- [21] Cambria E, White B. Jumping NLP Curves: A Review of Natural Language Processing Research [Review Article]. *IEEE Computational Intelligence Magazine*. 2014;9(2):48-57.
- [22] Devlin J, Chang M-W, Lee K, Toutanova K. BERT: Pre-training of Deep Bidirectional Transformers for Language Understanding. 2018.
- [23] Srivastava N, Goh H, Salakhutdinov R. Geometric Capsule Autoencoders for 3D Point Clouds. 2019.
- [24] Deprelle T, Groueix T, Fisher M, Kim VG, Russell BC, Aubry M. Learning elementary structures for 3d shape generation and matching. 2019.
- [25] Ankerst M, Kastenmüller G, Kriegel H-P, Seidl T. 3D Shape Histograms for Similarity Search and Classification in Spatial Databases. In: Güting RH, Papadias D, Lochovsky F, editors. *Advances in Spatial Databases*. Berlin, Heidelberg: Springer Berlin Heidelberg; 1999. p. 207-226.
- [26] Nguyen A, Le B. 3D point cloud segmentation: A survey. 2013 6th IEEE Conference on Robotics, Automation and Mechatronics (RAM)2013. p. 225-230.
- [27] Luciano L, Ben Hamza A. Deep learning with geodesic moments for 3D shape classification. *Pattern Recognition Letters*. 2018;105:182-190.
- [28] Qi CR, Su H, Mo K, Guibas LJ. Pointnet: Deep learning on point sets for 3d classification and segmentation. *Proceedings of the IEEE conference on computer vision and pattern recognition*. 2017. p. 652-660.
- [29] Zanuttigh P, Minto L. Deep learning for 3D shape classification from multiple depth maps. 2017 IEEE International Conference on Image Processing (ICIP)2017. p. 3615-3619.
- [30] Zhao Y, Birdal T, Deng H, Tombari F. 3D point capsule networks. *Proceedings of the IEEE/CVF Conference on Computer Vision and Pattern Recognition*. 2019. p. 1009-1018.
- [31] Fernandez-Labrador C, Chhatkuli A, Paudel DP, Guerrero JJ, Demonceaux C, Gool LV. Unsupervised learning of category-specific symmetric 3d keypoints from point sets. *Computer Vision—ECCV 2020: 16th European Conference, Glasgow, UK, August 23–28, 2020, Proceedings, Part XXV 16*: Springer; 2020. p. 546-563.

- [32] Zhang Z, Sun J, Dai Y, Zhou D, Song X, He M. A Representation Separation Perspective to Correspondence-Free Unsupervised 3-D Point Cloud Registration. *IEEE Geoscience and Remote Sensing Letters*. 2022;19:1-5.
- [33] Rempe D, Birdal T, Zhao Y, Gojcic Z, Sridhar S, Guibas LJ. Caspr: Learning canonical spatiotemporal point cloud representations. 2020.
- [34] Thomas N, Smidt T, Kearnes S, Yang L, Li L, Kohlhoff K, et al. Tensor field networks: Rotation-and translation-equivariant neural networks for 3d point clouds. 2018.
- [35] Arvo J. Fast random rotation matrices. *Graphics gems III (IBM version)*. Elsevier; 1992. p. 117-120. ISBN 978-0-1240-9673-8.